ARTICLE
Journal of Cellular Biochemistry 113:2474–2487 (2012)

Journal of Cellular Biochemistry

Reversal Effects of Pantoprazole on Multidrug Resistance in Human Gastric Adenocarcinoma Cells by Down-Regulating the V-ATPases/mTOR/HIF-1α/P-gp and MRP1 Signaling Pathway In Vitro and In Vivo

Min Chen,[1] Shu-Ling Huang,[1] Xiao-Qi Zhang,[1] Bin Zhang,[1] Hao Zhu,[1] Vincent W. Yang,[2] and Xiao-Ping Zou[1*]

[1]*Department of Gastroenterology, the Affiliated Drum Tower Hospital of Nanjing University, Medical School, Nanjing 210008, P.R. China*

[2]*Division of Digestive Diseases, Emory University School of Medicine, Atlanta, Georgia*

ABSTRACT

To investigate reversal effects of pantoprazole (PPZ) on multidrug resistance (MDR) in human gastric adenocarcinoma cells in vivo and in vitro. Human gastric adenocarcinoma cell SGC7901 was cultured in RPMI-1640 medium supplemented with 10% fetal bovine serum and antibiotics in a humidified 5% CO_2 atmosphere at 37°C. Adriamycin (ADR)-resistant cells were cultured with addition of 0.8 μg/ml of ADR maintaining MDR phenotype. ADR was used to calculate ADR releasing index; CCK-8 Assay was performed to evaluate the cytotoxicity of anti-tumor drugs; BCECF-AM pH-sensitive fluorescent probe was used to measure intracellular pH (pHi) value of cells, whereas pH value of medium was considered as extracellular pH (pHe) value; Western blotting and immunofluorescent staining analyses were employed to determine protein expressions and intracellular distributions of vacuolar H^+-ATPases (V-ATPases), mTOR, HIF-1α, P-glycoprotein (P-gp), and multidrug resistant protein 1 (MRP1); SGC7901 and SGC7901/ADR cells were inoculated in athymic nude mice. Thereafter, effects of ADR with or without PPZ pretreatment were compared by determining the tumor size and weight, apoptotic cells in tumor tissues were detected by TUNEL assay. At concentrations greater than 20 μg/ml, PPZ pretreatment reduced ADR releasing index and significantly enhanced intracellular ADR concentration of SGC7901 ($P < 0.01$). Similarly, PPZ pretreatment significantly decreased ADR releasing index of SGC7901/ADR dose-dependently ($P < 0.01$). PPZ pretreatment also decreased cell viabilities of SGG7901 and SGC7901/ADR dose-dependently. After 24-h PPZ pretreatment, administration of chemotherapeutic agents demonstrated maximal cytotoxic effects on SGC7901 and SGC7901/ADR cells ($P < 0.05$). The resistance index in PPZ pretreatment group was significantly lower than that in non-PPZ pretreatment group (3.71 vs. 14.80). PPZ at concentration >10 μg/ml significantly decreased pHi in SGC7901 and SGC7901/ADR cells and diminished or reversed transmembrane pH gradient ($P < 0.05$). PPZ pretreatment also significantly inhibited protein expressions of V-ATPases, mTOR, HIF-1α, P-gp, and MRP1, and alter intracellular expressions in parent and ADR-resistant cells ($P < 0.05$). In vivo experiments further confirmed that PPZ pretreatment could enhance anti-tumor effects of ADR on xenografted tumor of nude mice and also improve the apoptotic index in xenografted tumor tissues. PPZ pretreatment enhances the cytotoxic effects of anti-tumor drugs on SGC7901 and reverse MDR of SGC7901/ADR by downregulating the V-ATPases/mTOR/HIF-1α/P-gp and MRP1 signaling pathway. J. Cell. Biochem. 113: 2474–2487, 2012.

KEY WORDS: MULTIDRUG RESISTANCE; TRANSMEMBRANE pH GRADIENT; ATP-BINDING CASSETTE TRANSPORTER SUPERFAMILY; VACUOLAR H^+-ATPases; PANTOPRAZOLE SODIUM

Conflicts of interest: the authors declare that they have no competing interests.

Grant sponsor: National Science Foundation; Grant numbers: 81071816, 81101814; Grant sponsor: Fundamental Research Funds for the Central Universities; Grant number: 021414340018.

*Correspondence to: Xiao-Ping Zou, MD, PhD, Department of Gastroenterology, the Affiliated Drum Tower Hospital of Nanjing University, Medical School, Nanjing 210008, P.R. China. E-mail: zouxiaoping795@hotmail.com

Manuscript Received: 26 January 2012; Manuscript Accepted: 29 February 2012

Accepted manuscript online in Wiley Online Library (wileyonlinelibrary.com): 6 March 2012

DOI 10.1002/jcb.24122 • © 2012 Wiley Periodicals, Inc.

Gastric cancer is one of the most common malignancies of humans with a high incidence in East Asia, South America, and East Europe. While surgical resection remains the primary treatment, chemotherapy is sometimes beneficial in patients with advanced gastric carcinoma [Ajani, 1998]. However, effectiveness of chemotherapy is often thwarted by simultaneous resistance of tumor cells to multiple cytotoxic drugs, known as multidrug resistance (MDR) [Ozben, 2006]. Mechanisms involved in MDR include decreased drug accumulation in tumor cells, altered intracellular drug distribution, increased detoxification, diminished drug-target interaction, increased DNA repair, altered cell-cycle regulation, and uncoupled pathways linking cellular damage with apoptosis [Martinez-Lacaci et al., 2007; Gillet and Gottesman, 2010].

Although MDR have several causes, one major form of resistance to chemotherapy has been correlated with three molecular "pumps" including P-glycoprotein (P-gp), multidrug resistant protein1 (MRP1), and breast cancer resistance protein (BCRP) [Szakacs et al., 2006]. Among them, the most prevalent of the MDR transporters are P-gp and MRP1, which can often be overexpressed in malignant cells and usually serve to pump anticancer drugs out of the cell, resulting in a reduction of intracellular drug levels necessary for effective therapy [Rees et al., 2009]. Admittedly, adriamycin (ADR) is one of the common substrates for P-gp and MRP1 [Okada et al., 2006]. It has been shown that P-gp and MRP1 can transport a variety of chemotherapeutics out of cancer cells and these transport proteins are often overexpressed in MDR tumors. Thus, one approach to improve treatment would be to inhibit expressions or functions of these transporters, thus restoring chemosensitivity to the tumor cells [Anuchapreeda et al., 2002; Norman et al., 2005].

Admittedly, Vacuolar H^+-ATPases (V-ATPases) represents a major mechanism in regulating transmembrane pH gradient [Nishi and Forgac, 2002; Jefferies et al., 2008]. Some human tumor cells, particularly those selected for MDR, exhibit increased V-ATPases activity, accelerating the acidity of intracellular vesicles, allowing drug sequestration and consequently promoting the MDR [Martinez-Zaguilan et al., 1993; Nishi and Forgac, 2002]. New insights into the mechanism of tumor acidification may provide new strategies targeting the inhibition of tumor acidification and V-ATPases are being investigated as a potential target in tumor treatment [Vaananen et al., 1990; Marquardt and Center, 1991]. mTOR, a serine/threonine protein kinase and target of rapamycin, acts as a primary regulator of protein synthesis and cell growth. According to previous findings, mTOR increases the translation of hypoxia-inducible factor 1α (HIF-1α) [Advani, 2010]. HIF-1α overexpression showed significantly induced expression of P-gp and MRP1, indicating that HIF-1α may confer hypoxia-induced drug resistance via reducing intracellular drug accumulation [Liu et al., 2008].

Proton pump inhibitors (PPIs) are inevitably mentioned in terms of acidification inhibition, and have enabled improvement of various acid-related disorders [Barrison et al., 2001]. In addition, PPIs have been identified as a potential chemosensitizer or an anti-tumor drug in chemotherapy [Luciani et al., 2004]. Tumor acidity may induce selective accumulation of PPIs in tumor tissues. By analogy with gastric compartment, PPIs may be protonated and transformed in active form in the acidic tumor microenvironment [De Milito and Fais, 2005ab]. The active ingredient in Pantoprazole (PPZ) sodium is a substituted bezimidazole, sodium 5-(difluoromethoxy)-2-{[(3,4-demethoxy-2-pyridinyl)methyl]sulfinyl}-1H-benzimidazole sesquihydrate, a compound that inhibits gastric acid secretion [De Milito and Fais, 2005a]. According to the study by Oostendorp et al. (2009), PPZ was chosen as the inhibitors of P-gp. Then we hypothesized that PPZ might inhibit the expressions of V-ATPases, mTOR, HIF-1α, P-gp, and MRP1, thereby contributing to reverse MDR of gastric cancer cells.

Consequently, our study aims to investigate whether PPZ could inhibit the acidification of tumor microenvironment, affects the transmembrane pH gradient, and reverse MDR of gastric cancer cells by inhibiting the V-H^+-ATPases/mTOR/HIF-1α/P-gp and MRP1 signaling pathway.

MATERIALS AND METHODS

REAGENTS AND DRUGS

Pantoprazole sodium salts (Altana Pharma AG D-78467 Konstanz, Germany) were resuspended in normal saline (0.85%) (1 mg/ml) immediately before use. Adriamycin (ADR) (KEYGEN Biotech, China. No. KGA8183) was diluted in phosphate-buffered saline (PBS) (2 mg/ml). *Cis*-diamminedichloroplatinum (Cisplatin, CDDP) (No. 7100361DC, Qilu Pharmo Co. Ltd, China) was resuspended in PBS (1 mg/ml) and stored at −20°C. 5-Fluorouracil (5-FU, No. 0710152, Jiangsu Hengrui Pharma. Co. Ltd, China) was added in solution (25 mg/ml) and stored at room temperature.

CELL CULTURE

Human gastric adenocarcinoma cell line (SGC7901) was a gift from Dr. Jing Sun from the department of oncology, the affiliated Drum Tower Hospital. The adriamycin-resistant SGC7901 (SGC7901/ADR) cells were kindly supplied by Dr. Ding Chen from KEYGEN Biotec, China. SGC7901/ADR cells were derived by stepwise selection with increasing ADR concentrations [Li et al., 2009]. SGC7901 cells were cultured in RPMI-1640 (Hyclone) supplemented with 10% Fetal Bovine Serum (FBS) (Hangzhou Sijiqing Biotec, Co. Ltd, China) and antibiotics (100 U/ml penicillin and 100 μg/ml streptomycin) in a humidified 5% CO_2 atmosphere at 37°C (Thermo). SGC7901/ADR cells were cultured in the same medium, except the addition of 0.8 μg/ml of ADR.

CYTOTOXIC ASSAY (CELL COUNT KIT, CCK-8 ASSAY)

The cytotoxicity of PPZ and/or chemotherapeutic drugs was determined by CCK-8 assay [Wang et al., 2008]. Cells (1×10^4/well) were plated in 100 μl of medium/well in 96-well plates.

Effects of PPZ on cell viability. After overnight incubation, PPZ was added at the final concentration of 0, 1, 10, 20, 50, and 100 μg/ml, and CCK-8 assay was performed 24 h later. Briefly, 10 μl of CCK-8 solution was added and cultivated for another 2 h. The plates were then shaken for 30 s and the absorbance at 450 nm was measured with microplate reader (Bio-rad), using wells without cells as blanks and untreated cells as negative control. Cell viability was calculated with the formula: percent viability (%) = (OD of drug-treated sample/OD of untreated sample) × 100%.

The optimal PPZ pretreatment duration. After PPZ treatment at a concentration of 20 μg/ml for 0 (the PPZ + chemo-1 group), 12 (the PPZ + chemo-2 group), or 24 h (the PPZ + chemo-3 group), 5-FU, ADR, and cisplatin were simultaneously added with the final dose of 2.5, 0.3, and 1 μg/ml (1×) [Geran et al., 1972; Wang et al., 2008], respectively. CCK-8 assay was then performed 24 h later to evaluate the optimal duration of PPZ pretreatment.

IC_{50} and resistance index (RI) analyses. Cells with or without 24-h PPZ pretreatment were cultured in medium containing ADR or cisplatin or 5-FU with various concentrations including 0.01×, 0.1×, 1×, 10× for another 24 h before CCK-8 assay [The concentrations of (1×) of 5-FU, ADR and cisplatin were 2.5, 0.3, and 1 μg/ml, respectively]. IC_{50} and RI were then calculated based on the following formula: RI = IC_{50} (SGC7901/ADR)/IC_{50} (SGC7901).

INTRACELLULAR ADR MEASUREMENT

Briefly, cells (2×10^5 cells per well) were seeded in six-well plates and pretreated with 1, 10, 20, 50, and 100 μg/ml PPZ for 24–36 h. Cells without PPZ pretreatment served as control. Thereafter, cells were treated with 10 μM ADR for 1 h. Cells were then trypsinized and harvested (for detection of ADR accumulation) or, alternatively, cultured in drug-free RPMI-1640 for another 1 h followed by trypsinization and harvesting (for detection of ADR retention). Fluorescence intensity of intracellular ADR was determined by flow cytometry. The wavelengths of excitation light and emission light were 488 and 575 nm [Hong et al., 2007]. The ADR releasing index of cells was calculated according to the following formula: the ADR releasing index = (accumulation value − retention value)/accumulation value.

INTRACELLULAR AND EXTRACELLULAR pH (pHi AND pHe) MEASUREMENTS

The pH standard buffer A consisted of 133 mM KCl, 7 mM Cholin Cl, 1 mM $CaCl_2$, 2 mM KH_2PO_4, 5 mM glucose, and 6 mM HEPES, and its pH was adjusted to 6.2, 6.4, 6.6, 6.8, 7.0, 7.2, 7.4, and 7.6, respectively. The buffer B contained 135 mM NaCl, 5 mM KCl, 1.8 mM $CaCl_2$, 0.8 mM $MgSO_4$, 5 mM glucose, and 10 mM HEPES, and the pH of buffer B was adjusted to 7.4. These two buffers were stored at 4°C. A 5 mM Nigericin (Alexia Biochemical) stock solution was stored at −20°C. The pH sensitive fluorescent probe 2′,7′-bis-(2-carboxyethyl)-5-carboxyfluorescein acetoxymethyl ester (BCECF-AM) (Beyotime, China) was dissolved in DMSO (5 mM) and stored at −20°C. The pHi was measured by the BCECF-AM probe as previously described [Xia et al., 1999; Luciani et al., 2004]. The pH standard curve needs to be established by following procedure. The cells (1×10^5 cells per well) were incubated for 24–36 h and washed twice (5 min each time) with the buffer B; then each group of the cells were incubated in buffer B containing 5 μM BCECF-AM for 1 h and washed twice (5 min each time) with the buffer B; then each group of the cells were incubated in buffer B containing 5 μM BCECF-AM for 1 h and washed twice with each given-pH buffer A. Thereafter, each group of cells was treated with 5 μM Nigericin dissolving in each given pH buffer A for 15 min. After above-described procedure, the cells in each group were trypsinzed and resuspended in 1 ml buffer A with graded pH. The BCECF fluorescent intensity was measured by flow cytometry (BD). The excitation wavelength was 490 nm and the emission wavelength was 530 nm. The bivariate correlation between the fluorescent intensity (at 490 nm wavelength) and the pH value of solution A was analyzed to establish the pH standard curve. After 0, 1, 10, 20, 50, and 100 μg/ml PPZ pretreatment for 24 h, the pHi value of the cells were measured as above-described, except that the solution A was replaced by the solution B without Nigericin. Fluorescent intensity was recorded and the pHi was calculated using the pHi standard curve. The pHe value of the culture medium was measured by pH211 calibration check microprocessor pH meter (HANNA Instrument, Italy).

WESTERN BLOTTING ANALYSES OF V-H^+-ATPases, mTOR, HIF-1α, P-gp, AND MRP1

Briefly, cells were lysed in lysis buffer [containing 0.01% phenylmethanesulfonyl fluoride (PMSF), 150 mmol/L sodium chloride, 50 mM Tris (pH = 8), 0.1% sodium dodecylsulfonate (SDS), 0.2% ethylenediaminetetraacetic acid (EDTA), 1% Triton X-100, 1% sodium deoxycholate] supplemented with protease inhibitors (aprotinin, leupeptin, phenylmethylsulfonyl fluoride, sodium orthovanadate; Roche, Switzerland) and incubated for 30 min on ice, and centrifuged at 12,000 rpm at 4°C for 15 min to remove the nuclei and cell debris [Ranta et al., 2008]. The protein concentration of the extracts was determined by bicinchoninic acid (BCA) Protein Assay Kit (KEYGEN, China), following the manufacturer's instructions. A total of 50 μg of each cell extract was electrophoresed by sodium dodecyl sulfate–olyacrylamide gel electrophoresis (SDS–PAGE) on 10% acrylamide and electroblotted to a nitrocellulose membrane using a semidry transfer system (Bio-Rad). Nonspecific binding was blocked by incubating the membrane in 1 × TBST (Tris-buffered saline containing 0.05% Tween-20) supplemented with 5% nonfat dry milk for 1 h. Blots were then incubated with the polyclonal mouse antibody to V-H^+-ATPase subunit V_1A (Taiwan Abonova, China) and HIF-1α (Abcam) (1:2,500 and 1:1,000 dilution, respectively), or the polyclonal rabbit antibodies to mTOR (Cell signal), P-gp and MRP1 (Santa Cruz) (1:2,000, 1:500, and 1:500 dilution, respectively), and a monoclonal mouse antibody to β-actin (1:3,000 dilution, Santa Cruz) as a internal control for protein loading. Antibody binding was detected by incubating the blot with a horseradish peroxidase-conjugated goat anti-mouse (1:1,000 dilution, KPL) or goat anti-rabbit antibody (1:2,000 dilution, Bioworld) for 1 h. Antibody staining was visualized by enhanced chemiluminescence (Santa Cruz). The images of Western blot products were analyzed by Quantity One V4.31 (Bio-Rad).

CELLULAR IMMUNOFLUORESCENT STAINING OF V-H^+-ATPases, mTOR, HIF-1α, P-gp, AND MRP1

Dispersed single cells (2×10^5 cells/well) were grown on $22 \times 22 \times 1$ mm^3 glass coverslips (coated with 0.3% gelatine) in six-well culture plates. After 36–48 h incubation, cells with or without 24-h PPZ pretreatment were fixed in ice-cold acetone for 10 min. The cells were blocked with 10% normal goat serum (Boster

Biotech, China) for 30 min and probed with the polyclonal mouse antibody to V-ATPases subunit V_1A and HIF-1α and the polyclonal rabbit antibodies to mTOR, P-gp, or MRP1 (1:100 dilution, respectively) at 4°C overnight. Alexa Fluor Dye Conjugated secondary antibodies (1:100 dilution, Alexa Fluor 488 goat anti-mouse IgG (H + L) highly cross-adsorbed and Alexa Fluor 594 goat anti-rabbit IgG (H + L) highly cross-absorbed, 2 mg/ml, Molecular Probes) were used to incubate for 1 h to visualize under a laser scanning confocal microscopy. Then the fluorescent quality was analyzed and compared by the software of Image Pro Plus 5.0, and the mean of integral optical density (IOD) was considered as the intensity of fluorescence.

EFFECTS OF PPZ AND/OR ANTI-TUMOR AGENTS ON TUMOR GROWTH IN VIVO

Solid tumor models were developed from the SGC7901 and SGC7901/ADR cells. Fifty-five male SCID immunodeficient BALB/C nude mice aged 4–6 weeks weighing 18–22 g (Model Animal Research Center of Nanjing University, SCXK 2005-002) were randomly divided into eleven groups (n = 5 each), and were kept in a germ-free environment and their food, water, and bedding were autoclaved prior to use. Twenty-five mice were subcutaneously injected with 3×10^6 SGC7901 cells resuspended in 0.2 ml of RPMI-1640 containing 10% FCS in the right scapcula, and other 25 mice with SGC7901/ADR cells. The rest five mice were taken as the normal group without receiving inoculation. Once tumors became evident (at least 0.30 cm × 0.30 cm, approximately 10 days after the tumor cell injection), PPZ resuspended in normal saline (15 mg/ml) immediately before use was orally administered by gavage [Watson and Smith, 2001] at a dose of 75 mg/kg. ADR was administered by intraperitoneal injection at a dose of 1.25 mg/kg [Azab et al., 2008] simultaneously with PPZ oral treatment, 24 h after PPZ treatment, or in mice that did not receive any PPZ treatment, or in mice that did only receive PPZ treatment, or in mice that even did not receive any treatment after inoculation. Tumor dimensions were measured once a day with calipers and body weight were also monitored. Tumor volume was estimated according to Geran et al. [1972] using the following formula: tumor volume (mm^3) = length (mm) × width^2 (mm^2)/2. The relative tumor volume or body weight was expressed as the V_t/V_0 or W_t/W_0 index, where V_t and W_t are the tumor volume or body weight on the day of measurement and V_0 and W_0 are the same indices at the start of the treatment. All mice were killed at the end of the experiments, within 3 weeks after the injection of the human tumor cells. Tumor specimens were fixed in 10% (v/v) neutral formalin solution for 24 h and processed routinely by embedding in paraffin. Tissue serial sections were cut at 4 μm. Then the TUNEL assay apoptotic cells in sections of mice tumor tissue were detected using an in situ apoptosis detection kit (KEYGEN, China) as instructed by the manufacturer. Cells were visualized with a light microscope (Olympus IX70, Japan). The apoptotic index was calculated as follows: the apoptotic index = number of apoptotic cells/total number of cells. The in vivo experiments strictly obeyed the ethical principles and guidelines for scientific experiments on animals.

STATISTICAL ANALYSIS

The data were presented as mean ± SD of three independent experiments at least. Statistical analyses were performed with the software package SPSS 13.0. The significant differences between the treated group and the control group were evaluated by one-way ANOVA, using Dunnett's method, whereas multiple comparisons between any two of the treated groups were performed using SNK and LSD methods following one-way ANOVA. One-way ANOVA with a pairwise multiple comparison procedure (Tukey test) was used to analyze the statistical significance of tumor volumes or tumor weights differences between the treatment groups in in vivo experiments carried out in tumor-bearing athymic mice. Statistical significance was defined as $P < 0.05$ for all tests.

RESULTS

CELL VIABILITY

Effects of different concentrations of PPZ on the viabilities of SGC7901 and SGC7901/ADR cells. A dose-dependent inhibitory effect of PPZ on the viabilities of SGC7901 and SGC7901/ADR cells were observed (Fig. 1A). There was no significant difference in cell viability among 0, 1, and 10 μg/ml groups ($P > 0.05$). However, significant differences were found in cell viability between any two of the 20, 50, and 100 μg/ml groups in the same cell types, and also between any of the three groups (20, 50, and 100 μg/ml) and any of the other three PPZ groups (0, 1, 10 μg/ml) ($P < 0.05$).

The optimal time of PPZ pretreatment. The results of combination strategy including PPZ and anti-tumor drugs were summarized in Figure 1B. The viabilities of the SGC7901 and SGC7901/ADR cells in the PPZ group, the chemo group, the PPZ + chemo group-1 (0 h), -2 (12 h), and -3 (24 h) were 88.77 ± 1.81% versus 91.04 ± 2.23%, 85.33 ± 1.77% versus 90.12 ± 1.33%, 71.57 ± 1.49% versus 74.07 ± 1.78%, 71.93 ± 0.94% versus 76.66 ± 1.33%, and 58.71 ± 1.18% versus 66.23 ± 0.96%, respectively. The cell viabilities in the last four groups were significantly lower than that in the PPZ group ($P < 0.01$). Meanwhile, the cell viabilities in the three PPZ + Chemo groups, especially in the PPZ + Chemo-3 group, also were significantly lower than that in the chemo group ($P < 0.01$).

Effects of PPZ pretreatment on reversing the MDR of SGC7901/ADR cells. Cell viability was assessed by CCK-8 assay after treatment with ADR and/or PPZ pretreatment in the two cell lines. The levels of cytotoxicity were indicated as the concentration that inhibits the response by 50%, IC_{50}. The IC_{50} values of ADR in SGC7901 and SGC7901/ADR were 1.24 ± 0.035 and 18.35 ± 0.084 μg/ml, respectively, and the resistance index, which was the ratio of IC_{50} value of the resistance cells to the IC_{50} of the sensitive cells, was 14.80, showing that SGC7901/ADR was more resistant to ADR than SGC7901 ($P < 0.05$). Meanwhile, the IC_{50} values of cisplatin in SGC7901 and SGC7901/ADR were 3.05 ± 0.034 and 6.73 ± 0.058, and that of 5-FU were 2.15 ± 0.036 and 5.69 ± 0.053 (μg/ml), respectively. However, after 24-h PPZ pretreatment followed by administration of ADR, the resistance indices (IC_{50} values of SGC7901 and SGC7901/ADR at 0.84 ± 0.022 and 3.12 ± 0.045 μg/ml, respectively) were significantly lower than that of the unpretreated cells (3.71 vs. 14.80) (Table I).

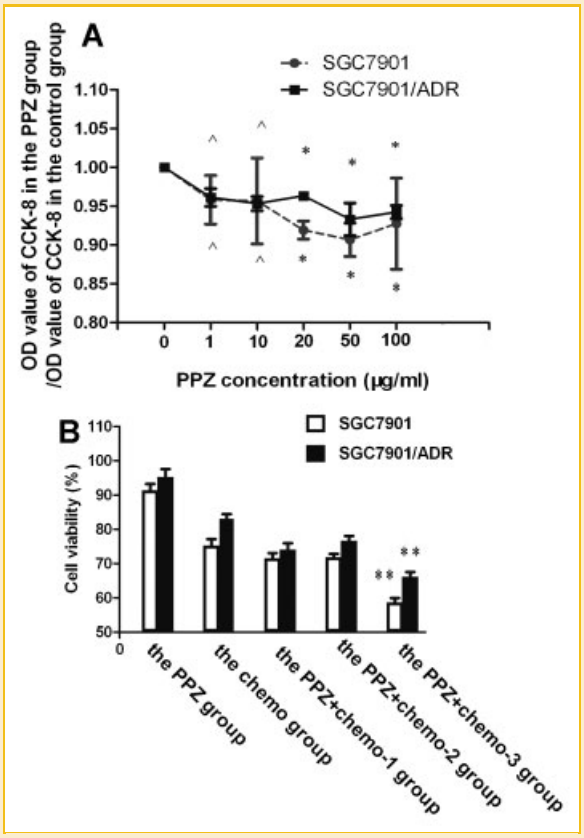

Fig. 1. A: Effects of 24-h PPZ pretreatment with different concentrations on the cell viabilities of SGC7901 and SGC7901/ADR. Notes: After 24-h incubation, cells were pretreated by PPZ with different concentrations for another 24 h. Then CCK-8 Assay was performed. A dose-dependent growth inhibition effect was observed after 24-h PPZ pretreatment including 0, 1, 10, 20, 50, and 100 μg/ml. All the experiments were conducted in triplicate, and the error bars represented the value of standard deviation (SD) of the mean. $^{\wedge}P > 0.05$ no significant difference was found in cell viability between any two of 0, 1, and 10 μg/ml PPZ groups. $^{*}P < 0.05$ significant differences were found in cell viability between any two of the 20, 50, and 100 μg/ml PPZ groups. There were significant differences in cell viability of any one of 20, 50, and 100 μg/ml PPZ groups when comparing to that in 0, 1, and 10 μg/ml PPZ groups. B: Comparison of the cell viability of SGC7901 and SGC7901/ADR after PPZ and/or anti-tumor drugs treatment. Notes: The PPZ group: After 48-h incubation, PPZ was added into cells. The chemo group: After 48-h incubation, ADR, 5-Fu, and cisplatin were added into cells (No PPZ pretreatment). The PPZ + chemo-1 group: After 48-h incubation, PPZ, ADR, 5-Fu, and cisplatin were simultaneously added into cells (No interval time between PPZ and chemotherapeutic drugs). The PPZ + chemo-2 group: PPZ was added into cells after 36-h culturing, and then at 48 h ADR, 5-Fu, and cisplatin were added into cells (PPZ pretreatment for 12 h). The PPZ + chemo-3 group: PPZ was added into cells after 24-h culturing and then at 48 h ADR, 5-Fu, and cisplatin were added into cells (PPZ pretreatment for 24 h). CCK-8 ASSAY was performed to detect the cell viability at 72 h. All the experiments were performed in triplicate. Dosage: PPZ (20 μg/ml); 5-Fu (2.5 μg/ml); cisplatin (1 μg/ml); ADR (0.3 μg/ml). $^{**}P < 0.01$ significant difference was found in cell viability between PPZ + Chemo-3 group and any one of the other four groups.

PPZ PRETREATMENT INCREASED INTRACELLULAR ADR ACCUMULATION IN SGC7901 AND SGC7901/ADR CELLS

As shown in Figure 2, PPZ pretreatment reduced the ADR releasing indices of SGC7901 and SGC7901/ADR. At a concentration higher than 20 μg/ml, PPZ reduced the ADR releasing index of SGC7901 significantly ($P < 0.01$). However, there was no significant difference between any two of the 20, 50, and 100 (μg/ml) PPZ groups ($P > 0.05$). Meanwhile, PPZ pretreatment significantly lowered ADR releasing index of SGC7901/ADR in a dose-dependent manner ($P < 0.01$). In addition, significant differences were found between any two of the five different-dosage PPZ groups in SGC7901/ADR ($P < 0.05$). Coincidently, PPZ pretreatment also could significantly enhance fluorescent intensity of ADR in SGC7901 and SGC7901/ADR as shown in Figure 2B–F ($P < 0.05$).

TABLE I. IC_{50} and Resistance Index (RI) of Different Drugs for SGC7901 and SGC7901/ADR Cells (Mean ± SD, μg/ml)

Cell line	ADR	CDDP	5-FU
SGC7901	1.24 ± 0.035	3.05 ± 0.034	2.15 ± 0.036
SGC7901/ADR	18.35 ± 0.084	6.73 ± 0.058	5.69 ± 0.053
RI	14.80	2.21	2.64
SGC7901 (PPZ)	0.84 ± 0.022		
SGC7901/ADR (PPZ)	3.12 ± 0.045		
RI	3.71		

$RI = IC_{50}$ (SGC7901/ADR)/IC_{50} (SGC7901).
PPZ concentration: 20 μg/ml.

MEASUREMENT OF THE INTRACELLULAR AND EXTRACELLULAR pH VALUES

The standard curve of pHi value was demonstrated in Figure 3A. According to regression analysis, the mathematic model was established as: $Y = 1610 + 1.53 \times 10^{-5} e^{2.83X}$, $R^2 = 0.9782$. Then the pHi values of SGC7901 and SGC7901/ADR with or without PPZ pretreatment were calculated accordingly.

The pHi and pHe values of SGC7901 and SGC7901/ADR at 0 h and at 24 h after PPZ pretreatment were shown in Figure 3B and C. The pHi values of the two cell lines at 0 h after PPZ pretreatment was 7.51 ± 0.05 versus 7.62 ± 0.07, and the pHe values at 0 h after PPZ pretreatment with different concentrations including 1, 10, 20, 50, and 100 μg/ml were higher than that in the control group After 24-h PPZ pretreatment with the concentration of 10, 20, 50, and 100 μg/ml, the pHi values of the two cell lines were significantly lower than that in the control group ($P < 0.05$), whereas the pHi values after PPZ pretreatment (1 μg/ml) were slightly higher than in the control group ($P > 0.05$). Conversely, the pHe values were higher than that in the control group.

The pH gradients in SGC7901 and SGC7901/ADR after 24-h PPZ pretreatment were demonstrated in Figure 3D and E. At 0 and 24 h after PPZ pretreatment with the concentrations of 0, 1, 10, 20, 50, and 100 μg/ml the pH gradients of SGC7901 were −0.11 versus −0.38, 0.1 versus −0.07, 0.11 versus 0.15, 0.17 versus 0.24, 0.25 versus 0.28, and 0.41 versus 0.52, respectively (Fig. 3D). In terms of SGC7901/ADR, the pH gradients were −0.4 versus −0.22, −0.45 versus −0.01, −0.29 versus 0, −0.17 versus 0.06, 0.01 versus 0.14, and 0.05 versus 0.10, respectively (Fig. 3E).

Meanwhile, changes of pH gradient in SGC7901 after 24-h PPZ pretreatment also were positively correlated with the PPZ concentration. The exponential relationship between them was revealed, following the formula: $Y = -0.332 \times e^{(-x/3.2486)} + 0.0671$,

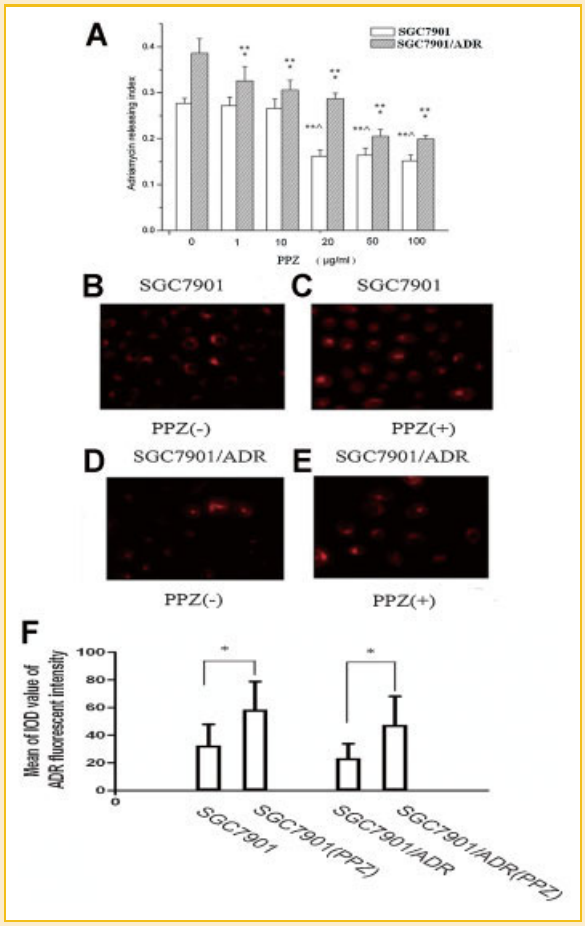

Fig. 2. Comparison of ADR releasing indices and ADR fluorescent intensity of SGC7901 and SGC7901/ADR with or without 24-h PPZ pretreatment. Notes: A: SGC7901 $^{**}P<0.01$ versus the control group (SGC7901). $^{\wedge}P>0.05$ no significant difference was found between any two of the three different-dosage PPZ groups. SGC7901/ADR $^{**}P<0.01$ versus the control group (SGC7901/ADR) $^{*}P<0.05$ significant difference was found between any two of the five different-dosage PPZ groups. B: ADR fluorescent intensity in SGC7901 without 24-h PPZ pretreatment (×200). The SGC7901 cells were incubated with RPMI-1640 containing ADR with the final concentration of 10 μM for 1 h and then were observed under a fluorescent microscope to detect the ADR fluorescent intensity. C: ADR fluorescent intensity in SGC7901 with 24-h PPZ pretreatment (20 μg/ml) (×200). After 24-h PPZ pretreatment with the concentration of 20 μg/ml, the SGC7901 cells were incubated with RPMI-1640 containing ADR with the final concentration of 10 μM for 1 h and then were observed under a fluorescent microscope to detect the ADR fluorescent intensity. D: ADR fluorescent intensity in SGC7901/ADR without 24-h PPZ pretreatment (×200). E: ADR fluorescent intensity in SGC7901/ADR with 24-h PPZ pretreatment (20 μg/ml) (×200). F: Then the fluorescent quality was analyzed and compared by the software of Image Pro Plus 5.0, and the mean of IOD was considered as the level of fluorescent intensity. The error bars represented the value of standard deviation (SD) of the mean. PPZ pretreatment also could significantly enhance fluorescent intensity of ADR in SGC7901 and SGC7901/ADR. $^{*}P<0.05$. [Color figure can be seen in the online version of this article, available at http://wileyonlinelibrary.com/journal/jcb]

$R^2=0.95022$ (Fig. 3F). However, changes of pH gradient in SGC7901/ADR after 24-h PPZ pretreatment also were negatively correlated with the PPZ concentration, following the formula: $Y=0.45843\times x^{(-0.28839)}$, $R^2=0.85116$ (Fig. 3G).

WESTERN BLOTTING ANALYSES OF V-ATPases, mTOR, HIF-1α, P-gp, AND MRP1 BEFORE AND AFTER PPZ PRETREATMENT (20 μg/ml)

The relative intensity values of V-H^+-ATPases of SGC7901 before and after PPZ pretreatment (20 μg/ml) were 0.49 ± 0.07 and 0.20 ± 0.02 ($P<0.05$), whereas those in SGC7901/ADR were 0.51 ± 0.04 and 0.39 ± 0.02 ($P<0.05$). Nevertheless, there is no significant difference in V-ATPases expression between SGC7901 and SGC7901/ADR ($P>0.05$). According to mTOR, the levels of SGC7901 before and after PPZ pretreatment were 0.41 ± 0.10 and 0.32 ± 0.08 ($P<0.01$), whereas those of SGC7901/ADR were 0.35 ± 0.09 and 0.15 ± 0.03 ($P<0.01$). The levels of HIF-1α before and after PPZ pretreatment were 1.43 ± 0.20 and 1.15 ± 0.16 ($P<0.05$), whereas those of SGC7901/ADR were 1.20 ± 0.23 and 0.89 ± 0.17 ($P<0.05$). As to P-gp, the relative intensity values of SGC7901 before and after PPZ pretreatment were 0.81 ± 0.05 and 0.15 ± 0.01 ($P<0.05$), whereas those of SGC7901/ADR were 1.03 ± 0.07 and 0.32 ± 0.03 ($P<0.05$). And the levels of P-gp of SGC7901/ADR were significantly higher than those of SGC7901 ($P<0.05$). When MRP1 was concerned, the relative intensity values of SGC7901 before and after PPZ pretreatment were 0.25 ± 0.05 and 0.16 ± 0.03 ($P<0.05$), whereas those of SGC7901/ADR were 0.86 ± 0.09 and 0.41 ± 0.07 ($P<0.05$). And the expressions of MRP1 of SGC7901/ADR were significantly higher than those of SGC7901 ($P<0.05$) (Fig. 4).

IMMUNOFLUORESCENT STAINING ANALYSES OF V-H^+-ATPases, mTOR, HIF-1α, P-gp, AND MRP1

PPZ pretreatment (20 μg/ml) resulted in a different intracellular expressions of V-H^+-ATPases, mTOR, HIF-1α, P-gp, and MRP1. After 24-h PPZ pretreatment, the intracellular expressions of V-H^+-ATPases, mTOR, HIF-1α, P-gp, and MRP1 expressions were relatively sparser and weaker compared to those before PPZ pretreatment. Therefore, the fluorescent intensity values of V-H^+-ATPases, mTOR, HIF-1α, P-gp, and MRP1 expressions after 24-h PPZ treatment also significantly decreased compared to those before PPZ pretreatment (Fig. 5).

EFFECTS OF PPZ ON SENSITIVITY OF HUMAN TUMORS TO ANTI-TUMOR AGENTS IN ATHYMIC MICE ENGRAFTED WITH THE SGC7901 AND SGC7901/ADR CELLS

The findings of our in vivo experiments further supported our results in vitro. These mice have proved useful in assessing the in vivo efficacy of local and systemic anti-tumor treatments of PPZ and ADR. Figure 6A and B shows the changes of relative body weight of athymic mice in the six groups, and Figure 6C and D revealed that the changes of relative tumor volume in the five groups. Moreover, Figure 6E and F provided the direct comparisons of tumor sizes in the five groups. According to these figures, it was shown that the relative tumor volume in the PPZ + ADR group (Interval) was the lowest, coincided with the results in vitro. The statistical data also were summarized in Table II. Figure 7 showed much more apoptotic cells of the tumor tissues in the PPZ + ADR group (Interval)

compared with the ADR group since there was a relatively higher apoptotic index in the PPZ + ADR group (Interval).

DISCUSSION

Recent years have witnessed more efforts in identifying agents to overcome MDR, contributing to improving effects of chemotherapy [Ford, 1996; de Jong et al., 2003]. Some chemosensitizers can modulate the resistance of tumors to chemotherapeutic drugs by affecting activity of plasma membrane transporter proteins of the ABC transporter family, which behave as energy-dependent efflux pumps for cytostatics [Angelini et al., 2007]. The two key mammalian transporters involved in transport of anticancer agents such as anthracyclines, are P-gp and MRP1. Results of our current study demonstrated that PPZ could overcome MDR of ADR-resistant SGC7901 by inhibiting protein expression of V-ATPases, mTOR, HIF-1α, P-gp, and MRP1 to a certain extent (Fig. 4).

Accumulating evidence indicate that PPIs have cytotoxic effects on various cancer cells. [Yeo et al., 2008] showed that PPZ might contribute to induction of apoptosis by inhibiting the phosphorylation of extracellular signal-regulated protein kinase 1/2 (ERK1/2) in gastric cancer cells. Thus it has been suggested that PPZ could be used for their selective anticancer effects, which might be caused by suppressing ERK phosphorylation. The proapoptotic activity of PPI was consistent with a clear inhibition of tumor growth following PPI treatment of B-cell lymphoma in severe combined immunodeficient mice. This study further supports the importance of acidity and pH gradients in tumor cell homeostasis and suggests new therapeutic approaches for human B-cell tumors based on PPIs [De Milito et al., 2007]. Recent studies indicate that the MDR1-gene product P-glycoprotein has considerable impact on bioavailability, tissue concentrations, and pharmacodynamic effects of drugs. Many drugs have been recognized to be substrates of this ATP-dependent efflux transporter whose activity can be enhanced or inhibited by various compounds [Pauli-Magnus et al., 2001]. According to the study by Pauli-Magnus et al. [2001], their data provide evidence that PPIs are substrates and inhibitors of P-glycoprotein, which might explain some of the drug interactions with PPIs observed in vivo. MIANS, a fluorescent probe sensitive to changes in microenvironment polarity of a protein molecule, has been used to study conformational changes in P-gp and MRP1 proteins. This feature allows specific labeling of accessible cysteine (Cys) residue on a protein, which leads to an increase in the MIANS fluorescence. Using the MIANS probe, many studies further confirmed that Cys residues were found in the NBDs of P-gp or MRP1. Thus it could be speculated that PPZ might inhibit the P-gp or MRP1 by combining the Cys residues locating in the NBDs of P-gp or MRP1 [Wan et al., 2009].

Our data indicate that PPZ at different concentrations significantly affect cell viability. According to Figure 1A, a dose-dependent growth inhibitory effect could be observed on the SGC7901 and SGC7901/ADR cells. We also found that simultaneous administration of PPZ and anti-tumor agents was less effective than administration of anti-tumor drugs after 24-h PPZ pretreatment. A possible explanation for this phenomenon may lie in a competition between the two drugs for the acidic tumor microenvironment. This competition may in turn lead, on one hand, to the inactivation of the cytotoxic drugs or, on the other hand, to the nonactivation of the PPZ, which needs to be protonated to work.

Our study also demonstrated that PPZ could significantly decrease ADR releasing index in the SGC7901 and SGC7901/ADR cells. SGC7901/ADR cells were selected with a single anticancer drug, ADR. So far, it has been used as a specific model for MDR research in gastric cancer since it exhibits simultaneous resistance to cisplatin and 5-FU, which respectively belongs to one of the structurally and functionally unrelated chemotherapeutic agents [Gillet and Gottesman, 2010]. Moreover, ADR was commonly used as a probe to evaluate drug accumulation and retention in cancer cells [Hong et al., 2007]. The ADR releasing index in SGC7901/ADR cells was significantly higher than that in SGC7901 cells, confirming the resistance of SGC7901/ADR cells to ADR. PPZ pretreatment decreased the ADR releasing index in a dose-dependent manner (Fig. 2). Additionally, SGC7901/ADR cells exhibited higher levels of P-gp and MRP1 than SGC7901 cells (Fig. 4). ADR is a common substrate for P-gp and MRP1 constituting well characterized mechanisms of MDR [Okada et al., 2006]. Since intracellular accumulation of ADR was obviously elevated after 24-h PPZ pretreatment, it could be predicted that P-gp and MRP1, as members of ABC transporter superfamily, which mediate energy-dependent drug efflux [Okada et al., 2006], might be inhibited by PPZ pretreatment. Thus it helped to explain why PPZ was able to reverse MDR of drug-resistant cells.

Fig. 3. A: Standard curve of fluorescent intensity of BECEF-AM versus the pHi value. Notes: The standard curve of pHi value was accordingly established. According to regression analysis, the mathematic model was established as: $Y = 1610 + 1.53 \times 10^{-5} e^{2.83X}$, $R^2 = 0.9782$. B: Comparison of extracellular and intracellular pH values of SGC7901 at 0 and 24 h after PPZ pretreatment with different concentrations. Notes: SGC7901 ^$P > 0.05$ no significant difference was found in the pHi value between the PPZ group (1 μg/ml) and the control group. *$P < 0.05$ significant differences were found in the pHi value between the PPZ group (10, 20, 50, and 100 μg/ml) and the control group. There were significant differences in the pHi value between any two of the 1, 10, 20, 50, and 100 μg/ml PPZ groups. *$P < 0.05$ significant differences were found in the pHe values after 0-h PPZ pretreatment and after 24-h PPZ pretreatment between the PPZ group (1, 10, 20, 50, and 100 μg/ml) and the control group. C: Comparison of extracellular and intracellular pH values of SGC7901/ADR at 0 and 24 h after PPZ pretreatment with different concentrations. Notes: SGC7901/ADR ^$P > 0.05$ no significant difference was found in the pHi value between the PPZ group (1 μg/ml) and the control group using Dunnett's method. *$P < 0.05$ significant differences were found in the pHi value between the PPZ group (10, 20, 50, and 100 μg/ml) and the control group using Dunnett's method. There were significant differences in the pHi value between any two of the 1, 10, 20, 50, and 100 μg/ml PPZ groups using SNK and LSD methods. *$P < 0.05$ significant differences were found in the pHe value after 0-h PPZ pretreatment between the PPZ group (1, 10, 20, 50, and 100 μg/ml) and the control group. Similar results also were found in the pHe value after 24-h PPZ pretreatment between the PPZ group (20, 50, and 100 μg/ml) and the control group. D: Comparison of pH gradients at 0 and 24 h after PPZ pretreatment with different concentrations in the SGC7901 cells. E: Comparison of pH gradients at 0 and 24 h after PPZ pretreatment with different concentrations in the SGC7901/ADR cells. F: Changes of pH gradient in SGC7901 after 24-h PPZ pretreatment with different concentrations. Notes: Changes of pH gradient = the pH gradient at 24 h after PPZ pretreatment − the pH gradient at 0 h after PPZ pretreatment. G: Changes of pH gradient in SGC7901/ADR after 24-h PPZ pretreatment with different concentrations.

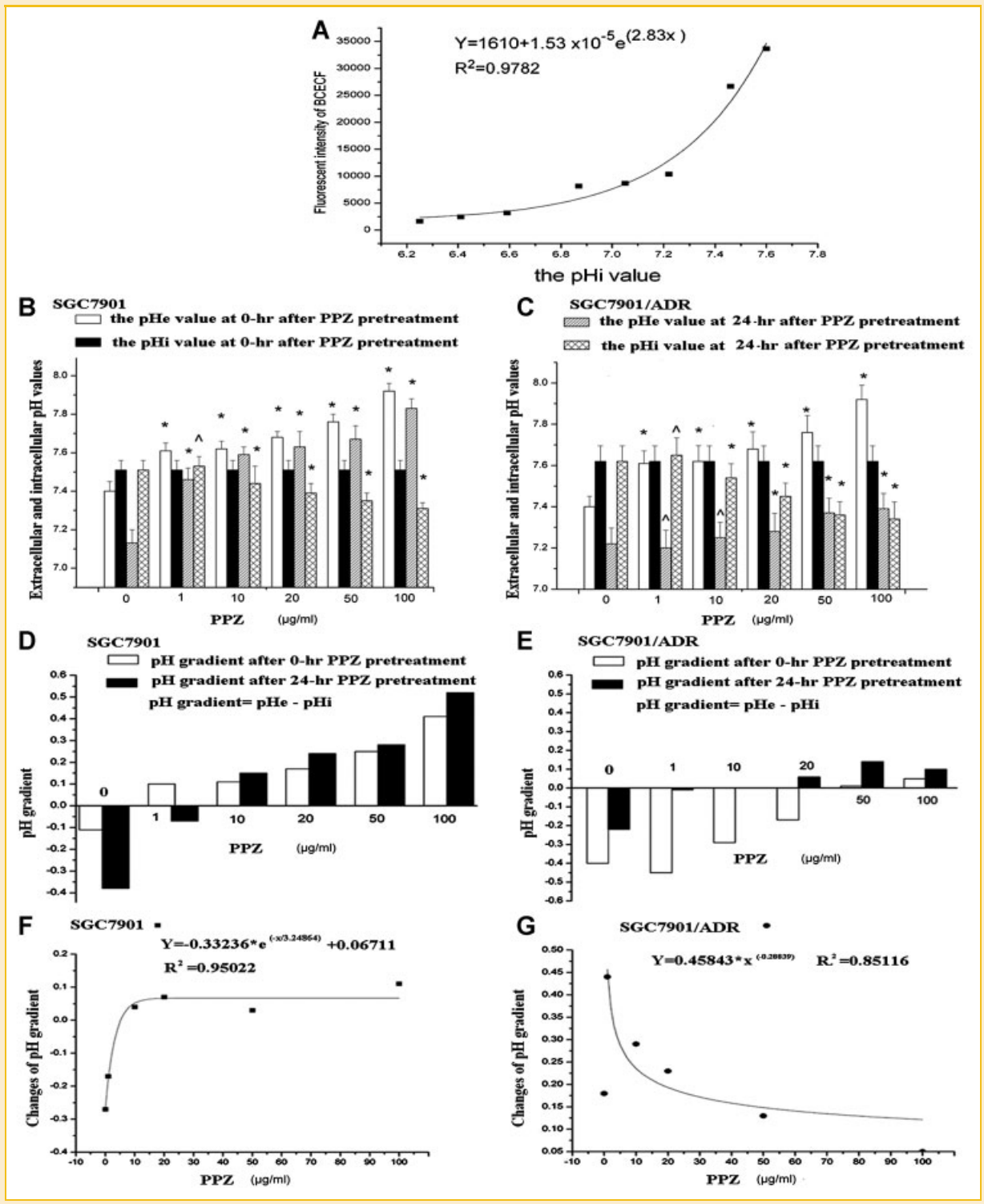
A
Y=1610+1.53 x10^-5 e^(2.83x)
R^2=0.9782
Fluorescent intensity of BCECF
the pHi value
B
SGC7901
the pHe value at 0-hr after PPZ pretreatment
the pHi value at 0-hr after PPZ pretreatment
Extracellular and intracellular pH values
PPZ (μg/ml)
C
SGC7901/ADR
the pHe value at 24-hr after PPZ pretreatment
the pHi value at 24-hr after PPZ pretreatment
Extracellular and intracellular pH values
PPZ (μg/ml)
D
SGC7901
pH gradient after 0-hr PPZ pretreatment
pH gradient after 24-hr PPZ pretreatment
pH gradient= pHe - pHi
pH gradient
PPZ (μg/ml)
E
SGC7901/ADR
pH gradient after 0-hr PPZ pretreatment
pH gradient after 24-hr PPZ pretreatment
pH gradient= pHe - pHi
pH gradient
PPZ (μg/ml)
F
SGC7901
Y=-0.33236*e^(-x/3.24864) +0.06711
R^2 =0.95022
Changes of pH gradient
PPZ (μg/ml)
G
SGC7901/ADR
Y=0.45843*x^(-0.28839)
R^2 =0.85116
Changes of pH gradient
PPZ (μg/ml)

Fig. 3.

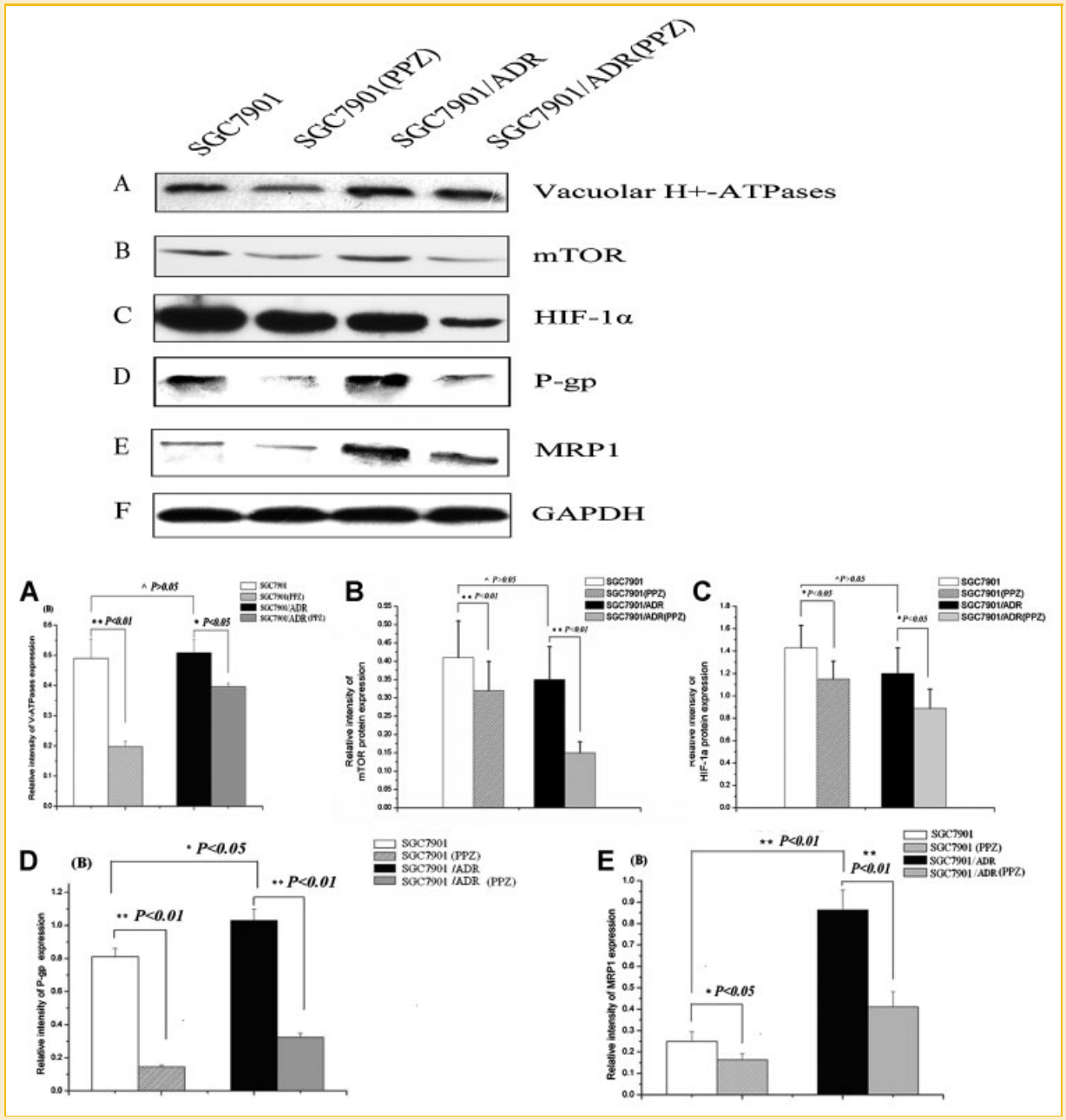

Fig. 4. Comparison of protein expressions of V-ATPases/mTOR/HIF-1α/P-gp and MRP1 in the SGC7901 and SGC7901/ADR cells with or without 24-h PPZ pretreatment. Notes: PPZ dosage: 20 μg/ml. $^{*}P < 0.05$; $^{**}P < 0.01$; $^{\wedge}P > 0.05$. A: Comparison of protein expressions of V-ATPases between with and without PPZ pretreatment in SGC7901 and SGC7901/ADR cells; B: comparison of protein expressions of mTOR between with and without PPZ pretreatment in SGC7901 and SGC7901/ADR cells; C: comparison of protein expressions of HIF-1α between with and without PPZ pretreatment in SGC7901 and SGC7901/ADR cells; D: comparison of protein expressions of P-gp between with and without PPZ pretreatment in SGC7901 and SGC7901/ADR cells; E: comparison of protein expressions of MRP1 between with and without PPZ pretreatment in SGC7901 and SGC7901/ADR cells.

Since our study aimed to investigate the role of PPZ as a chemosensitizer, we used a rather lower dosage to avoid its apoptosis-inducing effects and excessive alkaline pH value of PPZ solution. The concentration of PPZ exceeding 20 μg/ml significantly decreased ADR releasing index of the SGC7901 cells (Fig. 2). Therefore, 20 μg/ml was considered as the optimal dosage of PPZ in our study.

Subsequently, Western blot analyses of P-gp and MRP1 further supported our prediction. As demonstrated in Figure 4, after 24-h PPZ pretreatment (20 μg/ml), the relative intensity values of P-gp and MRP1 in drug-sensitive and -resistant cells significantly decreased when compared to those without PPZ pretreatment. Consistent with the results of Western blot, the fluorescent staining analysis also verified the inhibitory effects of PPZ on intracellular

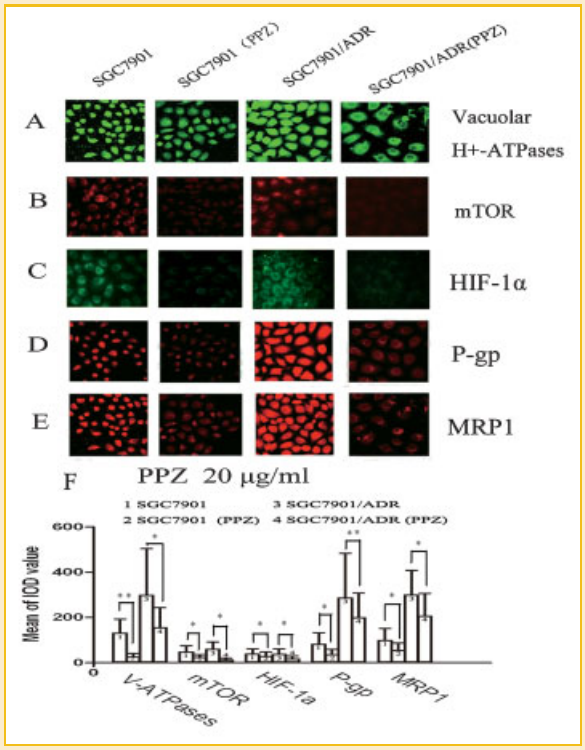

Fig. 5. Comparison of intracellular expressions of V-ATPases/mTOR/HIF-1α/P-gp and MRP1 in the SGC7901 and SGC7901/ADR cells with or without 24-h PPZ pretreatment via immunofluorescent staining (×400). Notes: PPZ dosage: 20 μg/ml. A: Comparison of intracellular expression of V-ATPases between with and without PPZ pretreatment in SGC7901 and SGC7901/ADR cells; B: Comparison of intracellular expression of mTOR between with and without PPZ pretreatment in SGC7901 and SGC7901/ADR cells; C: Comparison of intracellular expression of HIF-1α between with and without PPZ pretreatment in SGC7901 cells and SGC7901/ADR cells; D: Comparison of intracellular expression of P-gp between with and without PPZ pretreatment in SGC7901 and SGC7901/ADR cells; E: Comparison of intracellular expression of MRP1 between with and without PPZ pretreatment in SGC7901 and SGC7901/ADR cells. F: Then the fluorescent quality was analyzed and compared by the software of Image Pro Plus 5.0, and the mean of IOD was considered as the level of fluorescent intensity. The error bars represented the value of standard deviation (SD) of the mean. The fluorescent intensity values of V-H^+-ATPases, mTOR, HIF-1α, P-gp, and MRP1 expressions after 24-h PPZ treatment also significantly decreased compared to those before PPZ pretreatment. $^*P < 0.05$; $^{**}P < 0.01$. [Color figure can be seen in the online version of this article, available at http://wileyonlinelibrary.com/journal/jcb]

expressions of P-gp and MRP1 (Fig. 5). PPZ, admittedly, could inhibit function of various ATPases, induce the alterations of pHi homeostasis [Luciani et al., 2004], and then might indirectly influence the intracellular synthesis of ATP, providing the foundation for inhibiting the expression of energy-dependent ABC transporter superfamily.

PPZ pretreatment (20 μg/ml) also could inhibit expression of V-ATPases, involved in maintaining a relatively neutral pHi and an acidic pHe, through pumping protons into extracellular enviroment or lumen of some membrane-bound organelles [Nishi and Forgac, 2002; Jefferies et al., 2008]. Our results compared pH gradients before and after PPZ pretreatment (Fig. 3). The pH gradient with pHe less than pHi was altered into that with pHe more than pHi after PPZ pretreatment when PPZ concentration was more than 10 μg/ml in SGC7901 cells and more than 20 μg/ml in SGC7901/ADR cells. The study by Luciani et al. [2004] also suggested that PPZ is not only specific for reversing MDR of gastric cancer cells but also for several tumor cells including breast cancer, colon adenocarcinoma, ovarian adenocarcinoma, and melanoma cell lines. One reason could be explained that V-ATPases were highly expressed in those tumor cells.

Reversal of transmembrane pH gradient might play a certain role in reversing MDR of tumor cells. Unlike tumor pHi (which is neutral-to-alkaline) [Park et al., 1996], tumor pHe is often acidic [Larsen et al., 2000]. A pH gradient with pHe less than pHi disfavors uptake of weak base drugs [Prescott et al., 2000], and ADR (pH > 7.0) uptake is markedly decreased at low pHe since the charged form of the weak base drug is the protonated form, and it concentrates on the more acid side of membrane, leading to greater total drug on the acidic side of membrane. However, reversed pH gradient could effectively contribute to uptake of weakly basic anti-tumor drugs, enabling them to reach their intracellular target, thus increasing cytotoxicity. Therefore, accumulation of these drugs within tumor cells should also be affected by transmembrane pH gradient. Several studies [Keizer and Joenje, 1989; Li and Eastman, 1995] suggested that an acidic intracellular environment might greatly enhance effects of agents that cause apoptosis. As reported by Annette et al., changes in internal pH gradients were strongly associated with changes in drug distribution and sensitivity to anticancer agents [Larsen et al., 2000]. Interestingly, changes of pH gradient in SGC7901 after 24-h PPZ pretreatment were positively correlated with PPZ concentration in an exponential manner. However, changes of pH gradient in SGC7901/ADR after 24-h PPZ pretreatment were negatively correlated with PPZ concentration (Fig. 3). Why there are two distinctive kinds of relationships between them in the parent and resistant cells needs further investigation.

Alterations in pHi homeostasis have been implicated in drug resistance. MDR cells are sometimes observed with a more alkaline pHi than their drug-sensitive counterparts, yet this observation is inconsistent, indicating that other processes must be involved. According to our study, the pHi value of the SGC7901/ADR cells was higher than that of the SGC7901 cells, providing the reliable support (Fig. 3B and C).

In addition, PPIs are substituted 2-pyridyl-methylsulfinyl benzimidazoles sharing a similar core structure [Yeo et al., 2008] which are protonatable weak bases with a pKa (negative logarithm of the acid ionization constant) of approximately 4, with the exception of rabeprazole, which has a pKa of 5. Hence the active protonated form of PPIs will necessarily accumulate into acidic compartments. Therefore, it seemed conceivable that PPIs might specifically get to the tumor site, being an additional acidic compartment in cancer patients [De Milito and Fais, 2005a]. Since PPIs were weak base drugs as previously described, they could neutralize acid effluxing from tumor cells and maintain at a neutral or weak base extracellular microenvironment, enhancing cytotoxic effects of chemotherapeutics. As shown in Figure 3B and C, the pHe value also increased as the PPZ concentration improved.

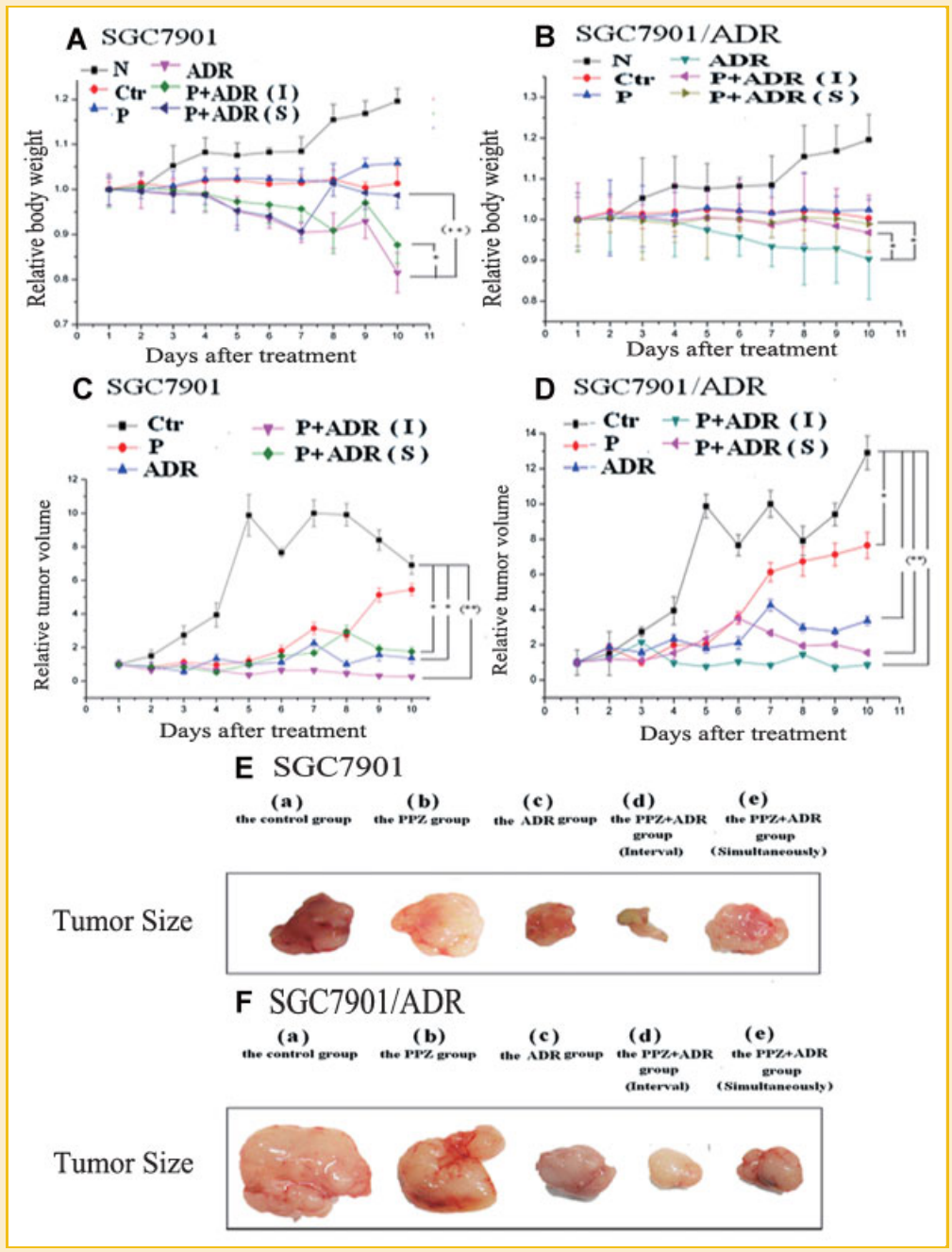

Fig. 6. A: Effects of PPZ and/or ADR on relative body weights of athymic mice xenografted with the SGC7901 cells.

Group	0 hour	24 hour (alternately)
1. The normal group (uninoculated)	no treatment	no treatment
2. The control group (inoculated and untreated)	no treatment	no treatment
3. The PPZ group	PPZ	Normal Saline (I.P.)
4. The ADR group	Normal Saline (Oral)	ADR
5. The PPZ+ADR group (interval)	PPZ	ADR
6. The PPZ+ADR group (simultaneously)	PPZ+ADR	Normal Saline (Oral and I.P.)

Dosage: PPZ 15 mg/ml 75 mg/kg Oral.

ADR 1 mg/ml 1.25 mg/kg I.P. * P<0.05; ** P<0.01.

B: Effects of PPZ and/or ADR on relative body weights of athymic mice xenografted with the SGC7901/ADR cells. $^{*}P < 0.05$. C: Effects of PPZ and/or ADR on relative tumor volume of athymic mice xenografted with the SGC7901 cells. $^{*}P < 0.05$; $^{**}P < 0.01$. D: Effects of PPZ and/or ADR on relative tumor volume of athymic mice xenografted with the SGC7901/ADR cells. $^{*}P < 0.05$; $^{**}P < 0.01$. E: Comparison of tumor sizes of athymic mice xenografted with the SGC7901 cells in the five groups; F: Comparison of tumor sizes of athymic mice xenografted with the SGC7901/ADR cells in the five groups. [Color figure can be seen in the online version of this article, available at http://wileyonlinelibrary.com/journal/jcb]

TABLE II. Effects of PPZ and/or ADR on Tumor Volume and Tumor Weight of Athymic Mice Xenografted With SGC7901 and SGC7901/ADR Before and After Treatment

Group (n = 5 in each group)	Tumor volume (mm^3)		Relative tumor volume	Rtv/ Ctv (%)	Tumor weight (g)	Inhibition rate (%)
	Start	End				
SGC7901						
The normal group	–	–	–	–	–	–
The control group	32.2 ± 7.92	210.0 ± 17.6	6.86	1	0.4805 ± 0.095	–
The PPZ group	62.5 ± 8.5	340.5 ± 21	5.45	79.4	0.4560 ± 0.065	5.1
The ADR group	56.7 ± 12.3	76.5 ± 17.5	1.35	19.7	0.2403 ± 0.059**	50.0
The PPZ + ADR group (Interval)	87.5 ± 10.3	22.5 ± 6.1	0.26	3.7	0.2058 ± 0.063**	57.2
The PPZ + ADR group (simultaneously)	75.3 ± 10.8	132.0 ± 19.7	1.75	25.5	0.2605 ± 0.074**	45.8
SGC7901/ADR						
The control group	55.4 ± 5.6	2025.0 ± 165.4	36.5	1	1.0057 ± 0.019	–
The PPZ group	53.8 ± 4.9	1470 ± 12.5	27.3	74.8	0.9413 ± 0.026	6.4
The ADR group	62.5 ± 5.8	280 ± 20.6	4.48	12.3	0.3701 ± 0.033**	63.2
The PPZ + ADR group (Interval)	48.5 ± 3.9	90.5 ± 23.4	1.87	5.1	0.2494 ± 0.019**	75.2
The PPZ + ADR group (simultaneously)	57.5 ± 4.6	150.5 ± 21.9	2.62	7.2	0.3047 ± 0.037**	69.7

Rtv/Ctv (%) = (relative tumor volume in treatment group/relative tumor volume in control group) × 100%.
Inhibition rate (%) = (tumor weight in control group − tumor weight in treatment group)/tumor weight in control group.
**$P < 0.01$ versus the control group.

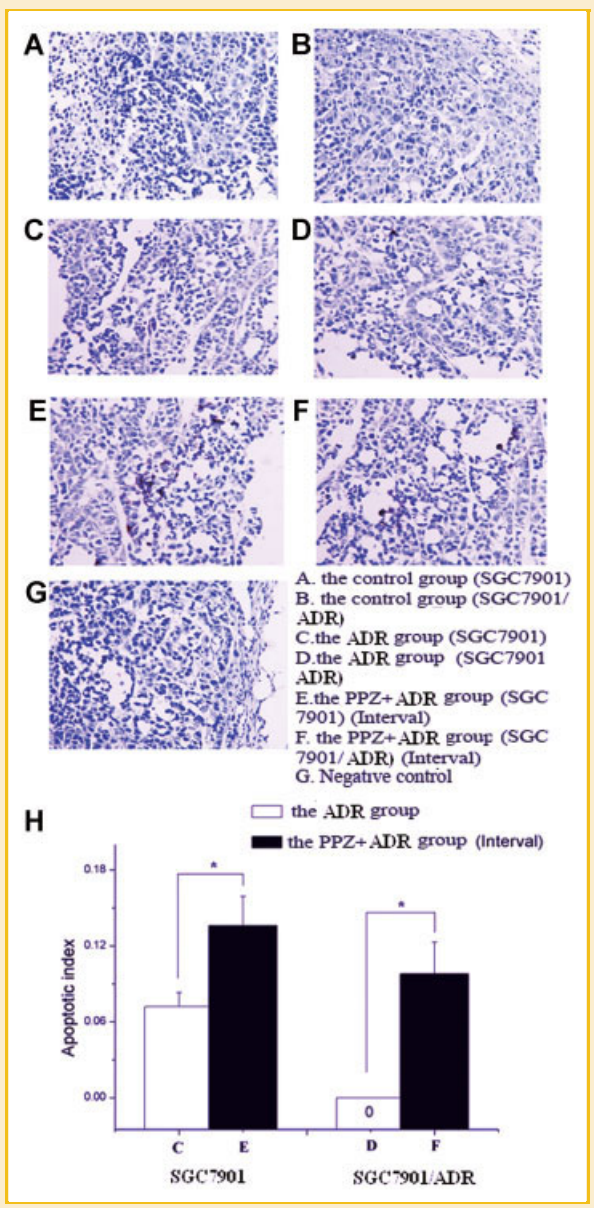

An important finding in our study was that PPZ pretreatment predisposed SGC7901/ADR cells to ADR, in which the mechanism of resistance is probably related to P-gp and MRP1 inconclusive. In our experiment, after 24-h PPZ pretreatment the resistance index decreased from 14.80 to 3.71.

Our in vivo experiments further confirmed the results of in vitro experiments. Both the relative tumor volume and tumor weight in the PPZ + ADR group (Interval) were the lowest when comparing to those in the other four groups, however, the apoptotic index in the same group also was significantly higher than that in the ADR group, hence hinting the synergetic effects of PPZ and ADR (Figs. 6, 7). As expected, the interval administration of PPZ and ADR showed higher anti-tumor efficacy and lower toxicity compared to the single administration of ADR, as shown by changes in relative tumor volumes, relative tumor weights and by immunohistological TUNEL assay data. Undoubtedly, there were several limitations in our study. One of the most important questions was that we had not conducted RNA interference technique to confirm the mutual relationship between any two of those proteins in the signaling pathway. Moreover, we also had not confirmed whether PPZ was specific for gastric cancer cells or not.

In conclusion, PPZ overcome the chemoresistance and enhance efficacy of chemotherapeutic drugs in SGC7901 and SGC7901/ADR cells by down regulating V-ATPases/mTOR/HIF-1α/P-gp and MRP1, suggesting that PPZ might play a critical role in chemotherapy in consideration of their low cost, minimal toxicity and high efficacy, modifying tumor pH gradients. Further preclinical and clinical trials are ongoing to provide the clinical

Fig. 7. Effects of ADR with or without PPZ pretreatment on the cell apoptosis in the SGC7901 or SGC7901/ADR tumor tissues by TUNEL assay (×400). A: The control group (SGC7901) (untreated); B: the control group (SGC7901/ADR) (untreated); C: the ADR group (SGC7901); D: the ADR group (SGC7901/ADR); E: the PPZ +ADR group (interval) (SGC7901); F: the PPZ +ADR group (interval) (SGC7901/ADR); G: negative control; H: effects of ADR with or without PPZ pretreament on the apoptotic index in the tumor tissues. The apoptotic index was calculated as follows: The apoptotic index = (number of apoptotic cells/total number) × 100%. *$P < 0.05$. [Color figure can be seen in the online version of this article, available at http://wileyonlinelibrary.com/journal/jcb]

proof of concept for the use of PPZ in the treatment of malignant cancers.

ACKNOWLEDGMENTS

This work was granted by National Science Foundation Grant no. 81071816 and no. 81101814 and simultaneously supported by the fundamental research funds for the central universities no. 021414340018. We also would like to express our gratitude to Prof. Runkuan Yang for his excellent revision on our manuscript.

REFERENCES

Advani SH. 2010. Targeting mTOR pathway: A new concept in cancer therapy. Indian J Med Paediatr Oncol 31:132–136.

Ajani JA. 1998. Chemotherapy for gastric carcinoma: New and old options. Oncology (Williston Park) 12:44–47.

Angelini A, Ciofani G, Baccante G, Di Febbo C, Carmine DI, Cuccurullo F, Porreca E. 2007. Modulatory effects of heparin on cellular accumulation and cytotoxicity of doxorubicin in MRP1-overexpressing HL60/doxo cells. Anticancer Res 27:351–355.

Anuchapreeda S, Leechanachai P, Smith MM, Ambudkar SV, Limtrakul PN. 2002. Modulation of P-glycoprotein expression and function by curcumin in multidrug-resistant human KB cells. Biochem Pharmacol 64:573–582.

Azab SS, Salama SA, Hassan MH, Khalifa AE, El-Demerdash E, Fouad H, Al-Hendy A, Abdel-Naim AB. 2008. 2-Methoxyestradiol reverses doxorubicin resistance in human breast tumor xenograft. Cancer Chemother Pharmacol 62:893–902.

Barrison AF, Jarboe LA, Weinberg BM, Nimmagadda K, Sullivan LM, Wolfe MM. 2001. Patterns of proton pump inhibitor use in clinical practice. Am J Med 111:469–473.

de Jong MC, Scheffer GL, Broxterman HJ, Hooijberg JH, Slootstra JW, Meloen RH, Kreitman RJ, Husain SR, Joshi BH, Puri RK, Scheper RJ. 2003. Multidrug-resistant tumor cells remain sensitive to a recombinant interleukin-4-Pseudomonas exotoxin, except when overexpressing the multidrug resistance protein MRP1. Clin Cancer Res 9:5009–5017.

De Milito A, Fais S. 2005a. Proton pump inhibitors may reduce tumour resistance. Expert Opin Pharmacother 6:1049–1054.

De Milito A, Fais S. 2005b. Tumor acidity, chemoresistance and proton pump inhibitors. Future Oncol 1:779–786.

De Milito A, Iessi E, Logozzi M, Lozupone F, Spada M, Marino ML, Federici C, Perdicchio M, Matarrese P, Lugini L, Nilsson A, Fais S. 2007. Proton pump inhibitors induce apoptosis of human B-cell tumors through a caspase-independent mechanism involving reactive oxygen species. Cancer Res 67:5408–5417.

Ford JM. 1996. Experimental reversal of P-glycoprotein-mediated multidrug resistance by pharmacological chemosensitisers. Eur J Cancer 32A:991–1001.

Geran RI, Greenberg NH, Macdonald MM, Shumacher AM, Abbot BJ. 1972. Protocols for screening chemical agents and natural products against animal tumors and natural other biological systems. Cancer Chemother Rep 3:1–88.

Gillet JP, Gottesman MM. 2010. Mechanisms of multidrug resistance in cancer. Methods Mol Biol 596:47–76.

Hong L, Wang J, Han Y, Zhao Y, Gao J, Zhang X, Yan L, Zhou X, Qiao T, Chen Z, Fan D. 2007. Reversal of multidrug resistance of vincristine-resistant gastric adenocarcinoma cells through up-regulation of DARPP-32. Cell Biol Int 31:1010–1015.

Jefferies KC, Cipriano DJ, Forgac M. 2008. Function, structure and regulation of the vacuolar (H+)-ATPases. Arch Biochem Biophys 476:33–42.

Keizer HG, Joenje H. 1989. Increased cytosolic pH in multidrug-resistant human lung tumor cells: Effect of verapamil. J Natl Cancer Inst 81:706–709.

Larsen AK, Escargueil AE, Skladanowski A. 2000. Resistance mechanisms associated with altered intracellular distribution of anticancer agents. Pharmacol Ther 85:217–229.

Li J, Eastman A. 1995. Apoptosis in an interleukin-2-dependent cytotoxic T lymphocyte cell line is associated with intracellular acidification. Role of the Na(+)/H(+)-antiport. J Biol Chem 270:3203–3211.

Li X, Sun B, Zhu CJ, Yuan HQ, Shi YQ, Gao J, Li SJ, Lou HX. 2009. Reversal of p-glycoprotein-mediated multidrug resistance by macrocyclic bisbibenzyl derivatives in adriamycin-resistant human myelogenous leukemia (K562/A02) cells. Toxicol In Vitro 23:29–36.

Liu L, Ning X, Sun L, Zhang H, Shi Y, Guo C, Han S, Liu J, Sun S, Han Z, Wu K, Fan D. 2008. Hypoxia-inducible factor-1 alpha contributes to hypoxia-induced chemoresistance in gastric cancer. Cancer Sci 99:121–128.

Luciani F, Spada M, De Milito A, Molinari A, Rivoltini L, Montinaro A, Marra M, Lugini L, Logozzi M, Lozupone F, Federici C, Iessi E, Parmiani G, Arancia G, Belardelli F, Fais S. 2004. Effect of proton pump inhibitor pretreatment on resistance of solid tumors to cytotoxic drugs. J Natl Cancer Inst 96:1702–1713.

Marquardt D, Center MS. 1991. Involvement of vacuolar H(+)-adenosine triphosphatase activity in multidrug resistance in HL60 cells. J Natl Cancer Inst 83:1098–1102.

Martinez-Lacaci I, Garcia Morales P, Soto JL, Saceda M. 2007. Tumour cells resistance in cancer therapy. Clin Transl Oncol 9:13–20.

Martinez-Zaguilan R, Lynch RM, Martinez GM, Gillies RJ. 1993. Vacuolar-type H(+)-ATPases are functionally expressed in plasma membranes of human tumor cells. Am J Physiol 265:C1015–C1029.

Nishi T, Forgac M. 2002. The vacuolar (H+)-ATPases—Nature's most versatile proton pumps. Nat Rev Mol Cell Biol 3:94–103.

Norman BH, Lander PA, Gruber JM, Kroin JS, Cohen JD, Jungheim LN, Starling JJ, Law KL, Self TD, Tabas LB, Williams DC, Paul DC, Dantzig AH. 2005. Cyclohexyl-linked tricyclic isoxazoles are potent and selective modulators of the multidrug resistance protein (MRP1). Bioorg Med Chem Lett 15:5526–5530.

Okada T, Tanaka K, Nakatani F, Sakimura R, Matsunobu T, Li X, Hanada M, Nakamura T, Oda Y, Tsuneyoshi M, Iwamoto Y. 2006. Involvement of P-glycoprotein and MRP1 in resistance to cyclic tetrapeptide subfamily of histone deacetylase inhibitors in the drug-resistant osteosarcoma and Ewing's sarcoma cells. Int J Cancer 118:90–97.

Oostendorp RL, Buckle T, Beijnen JH, van Tellingen O, Schellens JH. 2009. The effect of P-gp (Mdr1a/1b), BCRP (Bcrp1) and P-gp/BCRP inhibitors on the in vivo absorption, distribution, metabolism and excretion of imatinib. Invest New Drugs 27:31–40.

Ozben T. 2006. Mechanisms and strategies to overcome multiple drug resistance in cancer. FEBS Lett 580:2903–2909.

Park HJ, Makepeace CM, Lyons JC, Song CW. 1996. Effect of intracellular acidity and ionomycin on apoptosis in HL-60 cells. Eur J Cancer 32A:540–546.

Pauli-Magnus C, Rekersbrink S, Klotz U, Fromm MF. 2001. Interaction of omeprazole, lansoprazole and pantoprazole with P-glycoprotein. Naunyn Schmiedebergs Arch Pharmacol 364:551–557.

Prescott DM, Charles HC, Poulson JM, Page RL, Thrall DE, Vujaskovic Z, Dewhirst MW. 2000. The relationship between intracellular and extracellular pH in spontaneous canine tumors. Clin Cancer Res 6:2501–2505.

Ranta F, Dufer M, Stork B, Wesselborg S, Drews G, Haring HU, Lang F, Ullrich S. 2008. Regulation of calcineurin activity in insulin-secreting cells: Stimulation by Hsp90 during glucocorticoid-induced apoptosis. Cell Signal 20:1780–1786.

Rees DC, Johnson E, Lewinson O. 2009. ABC transporters: The power to change. Nat Rev Mol Cell Biol 10:218–227.

Szakacs G, Paterson JK, Ludwig JA, Booth-Genthe C, Gottesman MM. 2006. Targeting multidrug resistance in cancer. Nat Rev Drug Discov 5: 219–234.

Vaananen HK, Karhukorpi EK, Sundquist K, Wallmark B, Roininen I, Hentunen T, Tuukkanen J, Lakkakorpi P. 1990. Evidence for the presence of a proton pump of the vacuolar H(+)-ATPase type in the ruffled borders of osteoclasts. J Cell Biol 111:1305–1311.

Wan L, Liang X, Huang Y. 2009. Characterization of the ATPase activity of a novel chimeric fusion protein consisting of the two nucleotide binding domains of MRP1. Arch Biochem Biophys 485:102–108.

Wang J, Wang X, Jiang S, Lin P, Zhang J, Lu Y, Wang Q, Xiong Z, Wu Y, Ren J, Yang H. 2008. Cytotoxicity of fig fruit latex against human cancer cells. Food Chem Toxicol 46:1025–1033.

Watson SA, Smith AM. 2001. Hypergastrinemia promotes adenoma progression in the APC(Min−/+) mouse model of familial adenomatous polyposis. Cancer Res 61:625–631.

Xia QM, Huang J, Zhao ZQ, Qian GS. 1999. Fluorenscent measurements of intracellular pH in primary cultured inner medullary collecting duct cells of rabbit kidney. Acta Acad Med Militaris Tertiae 21:676–678.

Yeo M, Kim DK, Park HJ, Cho SW, Cheong JY, Lee KJ. 2008. Blockage of intracellular proton extrusion with proton extrusions with proton pump inhibitor induces apoptosis in gastric cancer. Cancer Sci 99:185.